Biogeochemistry (2020) 149:1–16
https://doi.org/10.1007/s10533-020-00656-9

Elevated nutrient inputs to marshes differentially impact carbon and nitrogen cycling in two northern Gulf of Mexico saltmarsh plants

Taylor C. Ledford · Behzad Mortazavi · Corianne Tatariw · Olivia U. Mason

Received: 11 October 2019 / Accepted: 9 March 2020 / Published online: 23 April 2020

Abstract Salt marsh biogeochemical processes are regulated by ecosystem structure (e.g. plant community composition). However, plant-specific responses to stressors such as elevated nutrient inputs can have differing impacts on nitrogen (N) removal and carbon (C) sequestration. We conducted a field manipulation to investigate the impact of elevated nutrient loading on ecosystem C dynamics and nitrate reduction pathways (denitrification and dissimilatory nitrate reduction to ammonium (DNRA)) in plots dominated by either *Juncus roemerianus* or *Spartina alterniflora* that were collocated in a northern Gulf of Mexico salt marsh. We increased N and phosphorus (P) inputs by two- and three-times current levels in the region. Nutrient enrichment had no effect on net ecosystem exchange. However, a three-fold increase in nutrient input resulted in nearly one-third increases in gross primary productivity (*GPP*) and ecosystem respiration in *S. alterniflora* plots, whereas there was no impact in *J. roemerianus* plots. Denitrification increased in *S. alterniflora* plots tenfold at both treatment levels relative to controls, but as with *GPP*, there was no response in *J. roemerianus* plots to higher nutrient inputs. In contrast, a three-fold increase in nutrients reduced DNRA by half in *J. roemerianus* plots. This work demonstrates that plant species-specific responses in marshes need to be considered for determining the impact of higher nutrient inputs on plant productivity and N-removal and retention.

Keywords *Juncus roemerianus* · *Spartina alterniflora* · Plant productivity · Net ecosystem exchange · Denitrification · DNRA

Responsible Editor: R. Kelman Wieder.

Electronic supplementary material The online version of this article (https://doi.org/10.1007/s10533-020-00656-9) contains supplementary material, which is available to authorized users.

T. C. Ledford · B. Mortazavi (✉) · C. Tatariw
Department of Biological Sciences, University of Alabama, 300 Hackberry Lane, Tuscaloosa, AL 35487, USA
e-mail: bmortazavi@ua.edu

O. U. Mason
Department of Earth, Ocean and Atmospheric Science, Florida State University, Tallahassee, FL 32306, USA

Introduction

Human activity has more than doubled the amount of reactive nitrogen (N) in the biosphere (Vitousek et al. 1997; Galloway et al. 2008). Activities such as industrial waste, sewage, and agricultural runoff associated with human population growth have been linked to high N inputs to rivers to coastal areas (Boesch 2002) contributing to global eutrophication of

N-limited coastal ecosystems such as estuaries, bays, and coasts (Nixon 1995; Rabalais et al. 2002; Smith 2003; Fabricius 2005; Howarth and Marino 2006; Smith et al. 2016). Salt marshes can reduce N inputs to coastal waters by burial and microbially mediated denitrification in addition to providing other ecosystem services such as flood control, erosion control, and carbon (C) sequestration (Valiela and Cole 2002; Fisher and Acreman 2004). Unfortunately, marshes are being lost at rates up to 2% per year (Bridgham et al. 2006) because of rising sea level, increased coastal development, and eutrophication with a subsequent loss in ecosystem services. Marsh restoration efforts such as the implementation of living shorelines (Bilkovic et al. 2016; Gittman et al. 2016) or constructing new marshes to replace lost surface area (Broome et al. 2019) are intended to mitigate the loss of ecosystem services. However, because biogeochemical cycles are tightly coupled to vegetation community composition (Alldred and Baines 2016), there is a need to better understand how plant species-specific responses to stressors such as eutrophication could mediate important processes such as N-removal.

Permanent N-removal in salt marshes is driven by the microbially-mediated process of denitrification, the step-wise reduction of nitrate (NO_3^-) to dinitrogen gas (N_2) (Knowles 1982). A competing microbial process that leads to the retention of N is dissimilatory nitrate reduction to ammonium (DNRA) (Burgin and Hamilton 2007), which makes up 25% − 50% of NO_3^- reduction in salt marsh sediments (Giblin et al. 2013). Vegetation composition can influence whether NO_3^- is removed or retained by altering organic matter (OM) quantity and quality (Hume et al. 2002; Babbin and Ward 2013), oxygen (O_2) translocation to the sediments (Koop-Jakobsen and Wenzhöfer 2015), and/or microbial community structure (Oliveira et al. 2010, 2012). Therefore, disturbances such as eutrophication that can impact plant productivity or composition could subsequently influence N-removal and/or N-retention.

We fertilized plots dominated by two common plants found in northern Gulf of Mexico marshes (*Spartina alterniflora* Loisel. and *Juncus roemerianus* Scheele.) to evaluate the importance of plant-specific responses in driving ecosystem carbon dioxide (CO_2) fluxes and denitrification/DNRA. Our study site is unique in that *J. roemerianus* and *S. alterniflora* are collocated, and there are minor elevation differences between species (Fig. 1), allowing us to examine plant-specific effects on C- and N-cycling in response to eutrophication.

Previous studies have shown that N-enrichment is more likely to favor *S. alterniflora* production than *J. roemerianus* production (Brewer 2003; Pennings et al. 2005; McFarlin et al. 2008), therefore we hypothesize a greater increase in *GPP* in *S. alterniflora* plots compared to *J. roemerianus* plots. While DNRA generally dominates in wetlands (Giblin et al. 2013), we predicted that with increased nutrient input and higher productivity, fertilization would promote denitrification over DNRA in both vegetation types, with a greater impact in the more N responsive *S. alterniflora.*

Methods

Study site

This study was conducted at a marsh located on the north side of Dauphin Island, AL, a subtropical barrier island 22.5 km in length and located in the northern central Gulf of Mexico at the terminus of Mobile Bay (30.2543 °N, 88.1124 °W, Fig. 1). The south side of the island consists of beaches exposed to the Gulf of Mexico, while the north side consists of brackish ponds and back-barrier marshes. This region receives − 2 kg N ha^{-1} y^{-1} via atmospheric deposition (National Atmospheric Deposition Program (NRSP-3) 2016) and the average annual temperature range is − 13 – 28 °C. Tides are diurnal with a mean tidal range of 0.36 m and averages salinity of − 27 PSU. This study site is unique as there is no clear vegetation zonation between *S. alterniflora* and *J. roemerianus*, which is typical of most mixed marshes. Alternatively, the dominant vegetation at the study site is *S. alterniflora* with patches of *J. roemerianus* well interspersed throughout (Fig. 1).

Experimental design

Boardwalks were installed at each study plot prior to the initiation of the project to minimize damage to the marsh. Nine plots per vegetation type were chosen randomly across *S. alterniflora* and *J. roemerianus* for a total of 18 plots. Only one vegetation type was present in each plot (*i.e. S. alterniflora* plots consisted

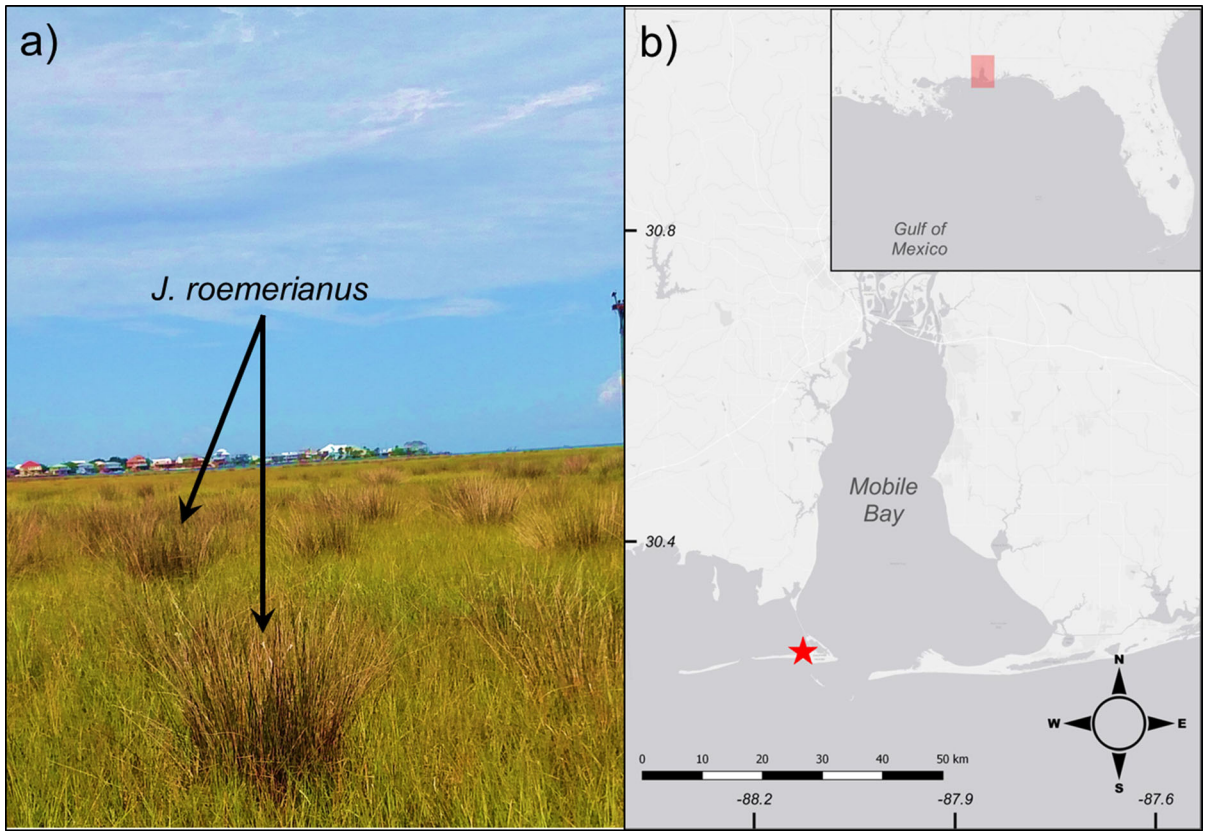

Fig. 1 **a** Image of study location on Dauphin Island, Alabama showing interspersion of *J. roemerianus* (indicated with arrows) within the *S. alterniflora* dominated marsh. **b** Map of study site location on Dauphin Island, Alabama, USA

only of *S. alterniflora*). In addition to three ambient control plots, triplicate plots for low nutrient inputs and high nutrient inputs were included for each vegetation type. To provide a realistic assessment of nutrient loading rates in the southeastern USA, high and low treatments were based on loading rates found in Mobile Bay, AL ($-$ 40 g N m^{-2} y^{-1} & $-$ 2.5 g P m^{-2} y^{-1}) and Ochlockonee Bay, FL ($-$ 20 g N m^{-2} y^{-1} and $-$ 1.25 g P m^{-2} y^{-1}), respectively (Twilley et al. 1999). For each nutrient application, sodium nitrate ($NaNO_3$) and monosodium phosphate (NaH_2PO_4) were mixed with filtered site water (Whatman GF/F, 1.2 µm) to desired concentrations and dispensed via garden sprayers (Project Source 1.5 L plastic tank sprayer) during low tide. Monthly fertilization treatments started in July 2017, two months prior to sampling events, and continued through August 2018. Experimental plots were separated by $\geq$ 1 m and enclosed in aluminum collars (0.26 m^2) to ensure adequate delivery of nutrients. Collars were embedded at 10 cm with holes at the sediment surface to allow natural drainage and inundation with the tidal cycle.

Site characteristics

Elevation was taken at each experimental plot with a RTK GPS (Trimble-R8 Model-3 rover Trimble® Real Time Kinematic (RTK) GPS and TSC-2 controller). Point measures of water column salinity, dissolved oxygen (DO), and water temperature were taken seasonally adjacent to marsh plots prior to each sampling period with a multiprobe (YSI model 556).

Above- and below-ground biomass was collected from *J. roemerianus* and *S. alterniflora* in areas outside of, but adjacent to, each experimental plot prior to fertilization to provide baseline comparisons. Above-ground biomass within a 0.024 m^2 quadrat was cut at the sediment surface. The vegetation was dried at 70 °C to a constant weight. Below-ground biomass

was collected with a metal T-corer (8.2 cm I.D.) inserted vertically to a depth of 15 cm. Cores were sectioned into 0–10 cm and 10–15 cm sections and wet sieved (2 mm). The collected below-ground biomass was then dried at 70 °C to a constant weight.

Sediment syringe cores (1.3 cm I.D.) from each experimental plot were taken seasonally to a 1 cm depth and dried to a constant weight to obtain porosity and bulk density. Dried sediments were ground and homogenized with a mortar and pestle. Carbonates were then removed from the sediment via acid fumigation with 12 N HCl for 24 h (Harris et al. 2001). Total sediment C and N was measured with a Costech Elemental Combustion System (Model 4010).

Separate sediment syringe cores (1.3 cm I.D.) from each experimental plot were taken seasonally to 5 cm depth for porewater extractable ammonium (NH_4^+). Homogenized sediment samples were extracted overnight on a shaker table with 2 M KCl (Smith and Caffrey 2009). Following the extraction, the supernatant was filtered through nylon membrane filter (VWR 0.45 µm pore size) and frozen until analysis. Ammonium (NH_4^+) concentrations were determined with a Turner Designs 7200–002 fluorometer equipped with a CDOM/NH4 UV module (Holmes et al. 1999).

Porewater analyses

Porewater sippers were installed permanently in each plot and allowed to equilibrate for at least 2 weeks prior to initiation of the study. Sippers were equipped with a porous window at 10 cm depth (Porex, 24–40 µm pore size), which allowed for porewater collection as described by Neubauer (2013). Sippers were purged of water and flushed with N_2 gas to remove oxygen prior to porewater collection. After 1 h, duplicate porewater samples were extracted, nylon membrane filtered into 15 mL centrifuge tubes, and stored on ice until returned to the lab where they were frozen until analysis. Samples were analyzed colorimetrically for concentrations of NO_x ($NO_3^- + NO_2^-$) and PO_4^{3-} using a UV–Vis spectrophotometer as described by previous methods (Grasshof et al. 1983; Schnetger and Lehners 2014). NH_4^+ concentrations were analyzed as described above (Holmes et al. 1999). Additional porewater samples were taken for H_2S analysis and placed in N_2 flushed 12 mL vacuum-sealed Exetainers (Labco, Lampeter, UK) with zinc acetate to preserve the sample. Samples were stored in the dark at room temperature until colorimetric analysis on a UV–Vis spectrophotometer (Fonselius et al. 1983).

Flux measurements

CO_2 fluxes were measured monthly with a transparent static chamber (0.26 m^2 × 1.02 m tall) placed on top of experimental plots as modified from Wilson et al. (2015). Holes in the side of the permanent collars were plugged with rubber stoppers and the edges of the collar were filled with water to provide an airtight seal. Within the phytochamber, three fans stirred the air and water was pumped through a heat exchanger to maintain an internal air temperature within ± 2 °C of ambient temperature. The chamber was allowed to equilibrate for 2 min before CO_2 concentrations were measured with a gas analyzer (LI-COR. Lincoln, NE, USA model LI-820) in line with the phytochamber. Measurements at full light were taken every second continuously for 2–3 min to obtain net ecosystem exchange (*NEE*). The chamber was then lifted to equilibrate with the atmosphere, and then resealed and darkened. CO_2 was re-measured in the dark to determine ecosystem respiration (ER_{CO_2}). Gross primary productivity was then calculated from the difference in *NEE* and ER_{CO_2}(Eq. 1), where *NEE* is the instantaneous flux into the marsh at full light and ER_{CO_2} is the flux out of the marsh in the dark.

$$GPP = NEE - ER_{CO_2} \quad (1)$$

Sampling was done during low tides on days with no rain and minimal cloud cover to allow for maximum light intensity.

Denitrification and anammox

Sediment cores (i.d. 2.6 cm) were collected from each experimental plot seasonally to a depth of 5 cm. Duplicate anoxic slurries were prepared from the sediment cores and artificial sea water (ASW) of a salinity consistent with the site water. Dinitrogen gas (N_2) was bubbled through the slurries to maintain anoxic conditions. Slurries were siphoned into 12 mL Exetainers (Labco), leaving no headspace. The Exetainer slurries were placed on a shaker table (− 70 rpm) in the dark overnight to draw down

residual NO_3^- and O_2 (Dalsgaard et al. 2005). Next, slurries were spiked to a concentration of 50 µM NO_3^- with $Na^{15}NO_3^-$ (98 atom%, Cambridge Isotope Laboratories, Inc.) then recapped with no headspace. Samples received 200 µL of 50% w/v $ZnCl_2$ to stop microbial activity at 0 h (t_0) and 6 h (t_f) following $^{15}NO_3^-$ addition. The production of $^{29}N_2$ and $^{30}N_2$ was measured on a membrane inlet mass spectrometer (MIMS) (Kana et al. 1994) with standard gas concentrations determined from Hamme and Emerson (2004). The mass spectrometer was equipped with an inline copper column heated to 600 °C to remove residual O_2 from samples (Eyre et al. 2002).

Denitrification rates from sediment slurries were determined from the isotope pairing technique as described by Nielsen (1992):

$$D_{15} = p29 + 2(p30), \tag{2}$$

where D_{15} represents denitrification of the added ^{15} N-NO_3^-, and $p29$ and $p30$ represent the rates of $^{29}N_2$ and $^{30}N_2$ production, respectively.

$$D_{14} = D_{15} \times \left[\frac{p29}{2 \times p30}\right], \tag{3}$$

where D_{14} represents denitrification of the ambient ^{14}N-NO_3^-. Equation (3) is used to account for any residual NO_3^- in the Exetainer after the drawdown incubation, though ambient concentrations were always low (< 2%).

$$D_t = D_{15} + D_{14}, \tag{4}$$

where D_t represents the total denitrification or potential dentrification capacity.

Potential anammox rates in sediment slurries were determined from Thamdrup and Dalsgaard (2002):

$$A_{total} = F_N^{-1} \times \left[P_{29} + 2 \times \left(1 - F_N^{-1}\right) \times P_{30}\right], \tag{5}$$

where A_{total} denotes production on N_2 through anammox, F_N is the fraction of ^{15} N in NO_3^-, and P_{29} and P_{30} represent the total produced mass of $^{29}N_2$ and $^{30}N_2$, respectively. Anammox was less than 2% of the total NO_3^- reduction for both vegetation types, and will not be discussed in this study.

DNRA

Additional duplicate slurries samples were set up as described above to determine potential DNRA rates. Following the addition of 200 µL of 50% w/v $ZnCl_2$, t_0 and t_f slurries were bubbled with N_2 gas to remove any $^{29}N_2$ and $^{30}N_2$ resulting from denitrification and/or anammox. Then, the $^{15}NH_4^+$ product of DNRA was converted to $^{29}N_2$ and $^{30}N_2$ using an alkaline sodium hypobromite solution. Samples were analyzed on a MIMS for isotopic dinitrogen gas, and potential DNRA rates were determined using methods described by Yin et al. (2014):

$$R_{DNRA} = \frac{\left[{}^{29+30}N_2\right]_{final} \times V - \left[{}^{29+30}N_2\right]_{initial} \times V}{W \times T}, \tag{6}$$

where R_{DNRA} denotes the total, measured ^{15} N-based potential DNRA rates, $[^{29+30}N_2]_{initial}$ and $[^{29+30}N_2]_{final}$ represent concentrations of $^{15}NH_4^+$ in the initial and final samples of the slurry experiments, respectively, V is the volume (L) of the incubation vial, W denotes the dry weight (kg) of the sediment, and T is the duration of the incubation (h).

Statistical analyses

N-cycle dynamics (denitrification and DNRA), CO_2 flux measurements (*GPP*, *NEE*, and ER_{CO_2}), porewater chemistries (NO_x, PO_4^{3-}, and NH_4^+), and sediment characteristics (total C:N, chlorophyll-a, and porewater extractable ammonium) in control plots (n = 3) were tested with a 1-way ANOVA with vegetation type as a fixed factor using R with the NLME package (R core team; Pinheiro et al. 2018). Response to nutrient input was tested within each vegetation type (i.e., treatments were not compared between vegetation types) using a 2-way ANOVA on linear mixed effects models (n = 3) where fertilization treatment and month were included as fixed effects and plot location was treated as a random effect. A first-order autoregressive (AR(1)) covariance structure was estimated to characterize the correlation of time-dependent data, and the model with the lowest Akaike information criterion (AIC) value was used. Below-ground biomass, above-ground biomass and sediment porosity (n = 3) were analyzed with a 1-way ANOVA with vegetation type as the factor (Car package, R core team; Fox and Weisberg 2011). Plot-specific differences were determined with a Tukey's HSD or Kruskal–Wallis test when data were nonparametric. Normality and homoscedasticity were tested

by visually inspecting plotted residuals. Equality of variances were tested with a Levene's test (Car package; R core team; Fox and Weisberg 2011). ANOVA results are reported unless otherwise stated.

Results

Site characteristics

Midday air temperatures at the study site ranged from 10.0 °C in March 2018 to 28.7 °C in July 2018. Soil temperatures ranged from 8.9 °C in January 2018 to 30.6 °C in June 2018. Porewater salinity ranged from ~ 12 PSU to ~ 29 PSU over the study period with no significant differences between species ($F_{(1,68)} = 3.393$, $p = 0.0698$; Table 1). Elevation was statistically different for *J. roemerianus* and *S. alterniflora* plots ($p < 0.05$) across all plots with respect to NAVD88, though all plot elevations were within 3 cm of each other (Table 1). Prior to treatment, total aboveground biomass was 87% higher in patches of *J. roemerianus* than patches of *S. alterniflora* ($F_{(1,3)} = 47.8$, $p = 0.002$; Table 1), and belowground biomass was 63% higher in patches of *J. roemeranus* than *S. alterniflora* ($F_{(3,15)} = 27.2$, $p < 0.05$; Table 1).

Sediment characteristics

Both sediment C:N and sediment C content were higher in *S. alterniflora* control plots compared to *J. roemerianus* ($F_{(1,16)} = 5.8$, $p = 0.03$ and $F_{(1,31)} = 5.5$, $p = 0.03$, respectively; Table 2). However, there was no difference in porewater extractable NH_4^+ concentrations ($F_{(1,22)} = 0.1$, $p = 0.77$; Table 2) between *J. roemerianus* and *S. alterniflora* control plots. There was no effect of fertilization treatment on sediment C:N, C content, or porewater extractable NH_4^+ concentrations in either vegetation type.

Porewater analyses

Porewater H_2S was, on average, 6X higher in *S. alterniflora* control plots than *J. roemerianus* control plots (1582.0 μM ± 191.4 SE and 261.0 μM ± 48.4 SE, respectively; $F_{(1,76)} = 20.2$, $p < 0.05$; Fig. 2). Otherwise, porewater NO_x, porewater NH_4^+, and porewater PO_4^{3-} concentrations were comparable in *J. roemerianus* and *S. alterniflora* control plots (NOx: $F_{(1,73)} = 1.2$, $p = 0.27$; NH_4^+: Kruskal–Wallis; Chi-squared = 16.542, df = 1, $p < 0.05$; PO_4^{3-}: $F_{(1,74)} = 0.2$, $p = 0.07$; Table 3).

There was no effect of fertilization treatment on porewater H_2S for either vegetation type ($F_{(2,71)} = 2.9$, $p = 0.63$ and $F_{(2,75)} = 2.9$, $p > 0.05$ for *J. roemerianus* and *S. alterniflora* plots, respectively; Fig. S1), but H_2S concentrations did vary temporally with highest concentrations in fall and winter in both vegetation types (October–December in *J. roemerianus* plots: $F_{(12,71)} = 3.6$, $p < 0.05$; October–January in *S. alterniflora* plots: $F_{(12,75)} = 10.4$, $p < 0.05$; Fig. S1). There was also no effect of fertilization on porewater NO_x for either vegetation type (*J. roemerianus*: $F_{(2,66)} = 1.965$, $p = 0.0148$; *S. alterniflora*: $F_{(2,66)} = 0.083$, $p = 0.920$), or porewater PO_4^{3-}

Table 1 Site characteristics taken from Airport Marsh prior to fertilization

	J. roemerianus	*S. alterniflora*
Belowground biomass (kg m^{-2})	4.64 ± 0.35a	2.84 ± 0.15b
Aboveground biomass (kg m^{-2})	12.09 ± 0.76a	6.46 ± 0.30b
Elevation (cm)	9.71 ± 0.52a	6.51 ± 0.27b
% total C	12.64 ± 0.37a	14.36 ± 0.62b
% total N	0.95 ± 0.03a	0.90 ± 0.04a
Soil C:N (mol:mol)	15.7 ± 0.21a	18.70 ± 0.72b
Porosity	0.77 ± 0.01a	0.77 ± 0.01a

Below-ground biomass taken from 10 cores in each vegetation type and averaged over 15 cm depth. Above-ground biomass is the total weight per unit area collected from each vegetation type (n = 3)

Values represent averages ± 1 standard error. Different letters indicate statistical differences between vegetation types ($p < 0.05$)

Table 2 Sediment concentrations of extracted ammonium (NH_4^+), total sediment C, and sediment C:N ratios collected seasonally concurrent with N-cycle dynamics (n = 3)

Vegetation type	2017–2018 season	Fertilization treatment	NH_4^+ (nmol g^{-1} dry weight)	Sediment C (%)	Sediment C:N (mol:mol)	Vegetation C:N (mol:mol)
J. roemerianus	Fall	Ambient	68.5 ± 14.2	12.3 ± 0.5	15.5 ± 0.3	–
		Low	73.6 ± 4.9	12.7 ± 1.0	15.5 ± 0.6	–
		High	121.0 ± 13.4	12.5 ± 1.3	15.1 ± 0.5	–
	Winter	Ambient	67.9 ± 13.8	13.5 ± 1.1	15.6 ± 0.6	–
		Low	86.2 ± 13.7	15.6 ± 1.8	18.0 ± 1.9	–
		High	50.3 ± 13.2	12.1 ± 1.6	16.9 ± 1.6	–
	Spring	Ambient	79.5 ± 28.5	13.3 ± 1.1	16.7 ± 1.2	54.8 ± 9.6
		Low	53.7 ± 10.6	14.3 ± 1.2	18.1 ± 1.5	43.6 ± 7.1
		High	82.0 ± 15.7	11.9 ± 1.0	17.0 ± 0.8	55.9 ± 5.6
	Summer	Ambient	48.4 ± 35.8	–	–	–
		Low	25.8 ± 4.6	–	–	–
		High	46.2 ± 4.3	–	–	–
S. alterniflora	Fall	Ambient	105.2 ± 21.5	14.9 ± 1.1	19.8 ± 1.9	–
		Low	111.5 ± 30.8	15.4 ± 0.5	19.1 ± 1.6	–
		High	111.9 ± 34.6	11.9 ± 1.9	18.5 ± 2.2	–
	Winter	Ambient	68.3 ± 7.0	15.2 ± 0.3	17.0 ± 0.6	–
		Low	105.0 ± 13.5	17.1 ± 0.6	16.0 ± 0.3	–
		High	52.9 ± 3.5	16.4 ± 0.3	16.5 ± 0.4	–
	Spring	Ambient	83.1 ± 17.7	15.4 ± 1.0	17.9 ± 1.6	33.8 ± 1.0
		Low	92.7 ± 17.3	14.8 ± 1.3	17.8 ± 1.1	30.9 ± 1.6
		High	50.8 ± 5.4	13.6 ± 1.1	17.7 ± 0.8	31.9 ± 0.9
	Summer	Ambient	26.0 ± 10.2	–	–	–
		Low	36.8 ± 3.7	–	–	–
		High	50.6 ± 11.6	–	–	–

Vegetation C:N was collected from shoots of *J. roemerianus* and *S. alterniflora* from treatment plots beginning in April 2018

Values represent averages ± 1 standard error

($F_{(2,71)} = 2.6$, $p > 0.05$ and $F_{(2,77)} = 0.1$, $p = 0.84$ for *J. roemerianus* and *S. alterniflora* plots, respectively). However, porewater NH_4^+ concentrations increased by 80% in fertilized *J. roemerianus* plots ($F_{(2,64)} = 7.0$, $p < 0.05$), and by nearly 40% in fertilized *S. alterniflora* plots ($F_{(2,70)} = 8.8$, $p < 0.05$).

CO_2 flux measurements

NEE and ER_{CO_2} did not differ between *J. roemerianus* and *S. alternilfora* control plots (Kruskal–Wallis, $p = 0.24$, $\chi^2 = 1.354$, df = 1, Fig. 3e, f; $F_{(1,63)} = 0.6$, $p = 0.44$; Fig. 3c and d). *GPP*, however, was marginally higher in *J. roemerianus* control plots compared to *S. alterniflora* control plots (20.6 µmol m^{-2} s^{-1} ± 2.1 SE and 19.6 µmol m^{-2} s^{-1} ± 1.4 SE, respectively; Kruskal−Wallis, $p = 0.05$, $\chi^2 = 3.7$, df = 1; Fig. 3a, b).

There was no effect of nutrient additions on *NEE* in either plant type, but it was always negative, indicating a net C sink (Fig. 3e, f). The only treatment effect on ER_{CO_2} occurred in the *S. alterniflora* high nutrient addition plots, where ER_{CO_2} increased nearly 30% ($F_{(10,66)} = 6.30$, $p < 0.05$; Fig. 3c, d). This respiration response was mirrored by nearly 30% increases in *GPP* in high addition *S. alterniflora* plots ($F_{(10,64)} = 12.12$, $p < 0.02$; Fig. 3b). There was no *GPP* response to nutrient additions in *J. roemerianus* plots (Fig. 3a).

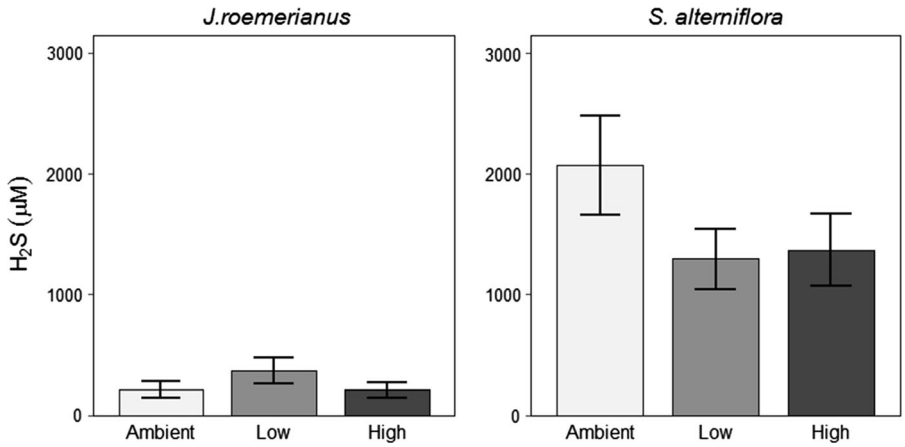

Fig. 2 Porewater H_2S concentrations (10 cm) from April 2017 to July 2018 in *J. roemerianus* and *S. alterniflora* patches (n = 3). Error bars indicate yearly averages ± 1 standard error. Vegetation types are significantly different (1-way ANOVA; $p < 0.05$)

Table 3 Seasonal porewater concentrations of hydrogen sulfides (H_2S), NOx (NO_3^- + NO_2^-), ammonium (NH_4^+), phosphate (PO_4^{3-}), and salinity collected over 2017–2018 study (n = 3)

Vegetation type	2017–2018 season	Fertilization treatment	Porewater H_2S (μM)	NO_x (uM)	NH_4^+ (uM)	PO_4^{3-} (uM)	Salinity (psu)
J. roemerianus	Fall	Ambient	454.0 ± 163.9	0.6 ± 0.2	111.7 ± 25.2	3.9 ± 1.5	26.8 ± 2.3
		Low	982.5 ± 219.9	0.6 ± 0.2	142.7 ± 25.6	5.5 ± 1.4	26.8 ± 1.0
		High	573.3 ± 157.6	0.9 ± 0.3	152.5 ± 27.8	5.1 ± 1.7	26.7 ± 1.3
	Winter	Ambient	212.6 ± 208.5	0.8 ± 0.2	52.4 ± 11.5	1.4 ± 0.5	24.1 ± 1.2
		Low	345.4 ± 337.8	2.4 ± 1.1	73.9 ± 15.1	4.2 ± 1.2	24.0 ± 1.3
		High	57.5 ± 57.5	3.5 ± 1.7	86.7 ± 24.2	2.9 ± 1.1	24.0 ± 0.7
	Spring	Ambient	16.4 ± 4.4	1.0 ± 0.4	30.3 ± 6.6	1.1 ± 0.3	24.1 ± 1.0
		Low	71.4 ± 28.0	1.2 ± 0.4	100.0 ± 30.8	2.0 ± 0.5	25.3 ± 1.8
		High	38.2 ± 36.6	0.9 ± 0.2	85.0 ± 24.9	0.6 ± 0.2	24.5 ± 1.3
	Summer	Ambient	277.0 ± 113.1	0.4 ± 0.2	16.0 ± 11.0	4.7 ± 1.3	20.0 ± 3.4
		Low	191.9 ± 72.7	0.8 ± 0.5	31.2 ± 15.2	5.1 ± 1.3	22.5 ± 2.8
		High	156.0 ± 147.7	0.8 ± 0.4	21.9 ± 10.8	4.2 ± 1.7	19.7 ± 2.9
S. alterniflora	Fall	Ambient	1700.4 ± 451.4	1.5 ± 0.4	201.5 ± 24.4	2.8 ± 0.3	21.3 ± 1.4
		Low	1694.8 ± 470.7	1.8 ± 0.6	256.7 ± 79.9	2.5 ± 0.4	21.7 ± 0.8
		High	1791.5 ± 520.7	1.1 ± 0.3	281.7 ± 73.7	3.7 ± 0.5	22.7 ± 0.6
	Winter	Ambient	3677.7 ± 1401.7	0.5 ± 0.1	161.5 ± 24.8	1.7 ± 0.4	22.2 ± 1.2
		Low	1276.5 ± 698.5	0.5 ± 0.2	115.9 ± 30.6	2.7 ± 0.8	23.3 ± 0.8
		High	2155.6 ± 976.5	0.4 ± 0.1	150.1 ± 42.8	1.7 ± 0.3	24.4 ± 0.5
	Spring	Ambient	777.1 ± 252.9	0.6 ± 0.2	150.7 ± 55.9	1.3 ± 0.2	22.6 ± 0.8
		Low	564.5 ± 241.7	0.7 ± 0.3	57.6 ± 22.0	1.2 ± 0.4	22.4 ± 0.9
		High	650.3 ± 286.6	0.8 ± 0.2	24.4 ± 9.4	0.8 ± 0.2	22.9 ± 1.0
	Summer	Ambient	2528.5 ± 711.2	1.6 ± 0.5	69.6 ± 29.0	2.5 ± 0.6	20.8 ± 0.5
		Low	2049.7 ± 677.5	0.8 ± 0.3	70.5 ± 33.6	2.9 ± 1.1	20.0 ± 0.7
		High	569.5 ± 182.1	1.4 ± 0.7	46.7 ± 17.3	3.7 ± 0.7	20.3 ± 1.0

Values represent averages ± 1 standard error

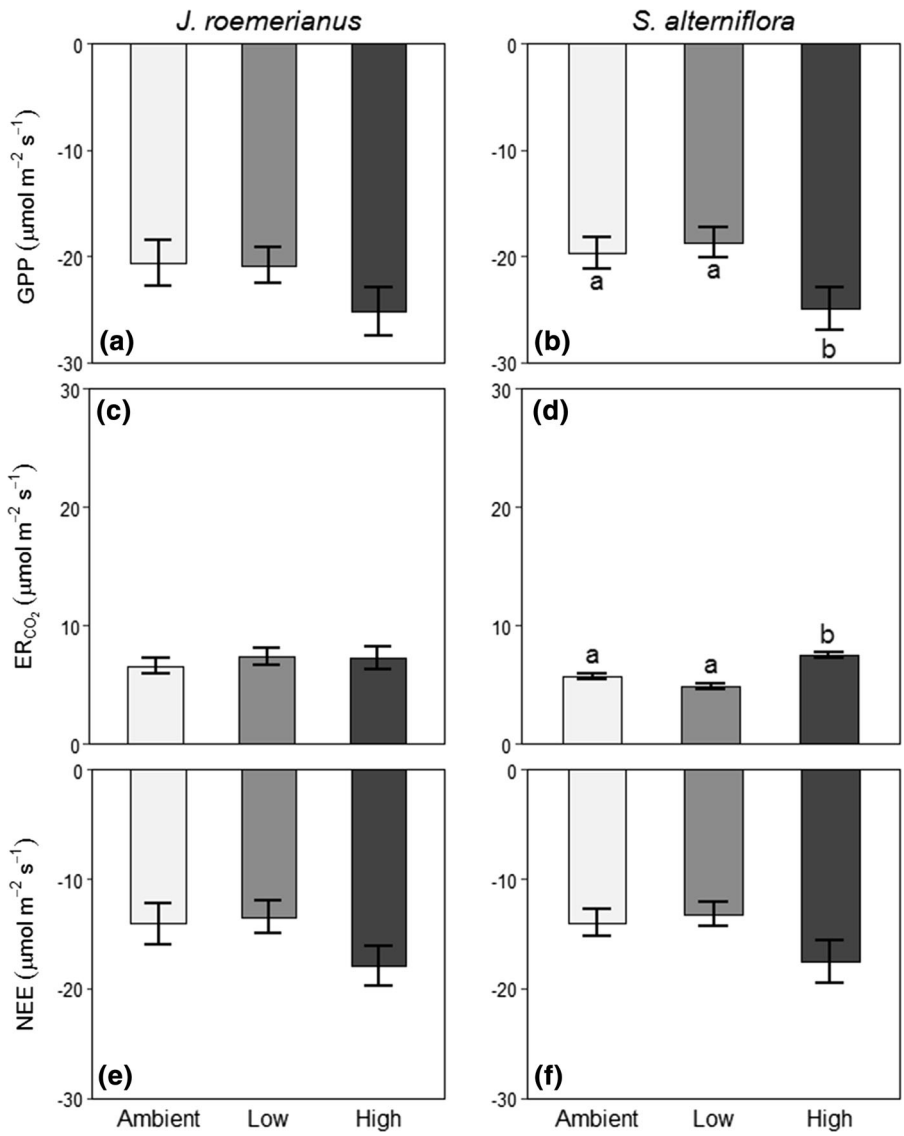

Fig. 3 CO_2 flux measurements for *GPP*,ER_{CO_2} and *NEE* in *J. roemerianus* (**a**, **c**, and **e**, respectively) and *S. alterniflora* patches (**b**, **d**, and **f**, respectively) (n = 3). CO_2 data were combined with environmental data taken from each sampling event. Error bars indicate yearly averages ± 1 standard error. *GPP* was marginally different between *J. roemerianus* and *S. alterniflora* ambient plots, but and *NEE* were similar (2-way ANOVA; $p > 0.05$). Different letters indicate significant differences between treatments (2-way ANOVA; $p < 0.05$)

In *J. roemerianus* plots, highest *NEE* was measured in October (33.0 ± 7.5 µmol m^{-2} s^{-1}; Fig. S2a, b), but was similar throughout the remainder of the year. In contrast, there was no temporal effect on *NEE* in *S. alterniflora* plots. The highest ecosystem respiration was measured in September and October for both vegetation types (*J. roemerianus*: 11.8 µmol m^{-2} s^{-1} ± 0.9 SE, $F_{(10,66)} = 3.648$, $p < 0.05$; *S. alterniflora*: 7.8 µmol m^{-2} s^{-1} ± 0.6 SE, $F_{(10,66)} = 2.976$, $p < 0.05$). Highest *GPP* was measured in October in *J. roemerianus* plots (44.8 µmol m^{-2} s^{-1} ± 4.7 SE; Fig. S2e, f), but otherwise did not vary throughout the study period. There was no temporal effect on *GPP* in *S. alterniflora* plots.

Nitrate reduction

Denitrification was nearly five times higher in control plots of *J. roemerianus* than in *S. alterniflora* control plots (31.9 μmol N kg^{-1} h^{-1} ± 6.8 SE and 6.4 μmol N kg^{-2} h^{-1} ± 3.4 SE, respectively; $F_{(1,22)}$ = 12.8, p = 0.002; Fig. 4a, b). However, DNRA was similar in *J. roemerianus* and *S. alterniflora* control plots (22.3 μmol N kg^{-1} h^{-1} ± 3.7 SE and 29.6 μmol N kg^{-1} h^{-1} ± 3.8 SE, respectively; $F_{(1,22)}$ = 1.9, p = 0.18; Fig. 4c, d).

Denitrification increased by ten-fold in in both low and high nutrient addition plots of *S. alterniflora* compared to controls ($F_{(2,24)}$ = 16.8, $p < 0.05$; Fig. 4b), while rates were similar across all *J. roemerianus* plots ($F_{(2,24)}$ = 2.1, p = 0.14; Fig. 4a). Unlike *GPP*, ER_{CO_2} and denitrification, DNRA did not respond to low or high nutrient additions in *S. alterniflora* plots, but declined by nearly 55% in high

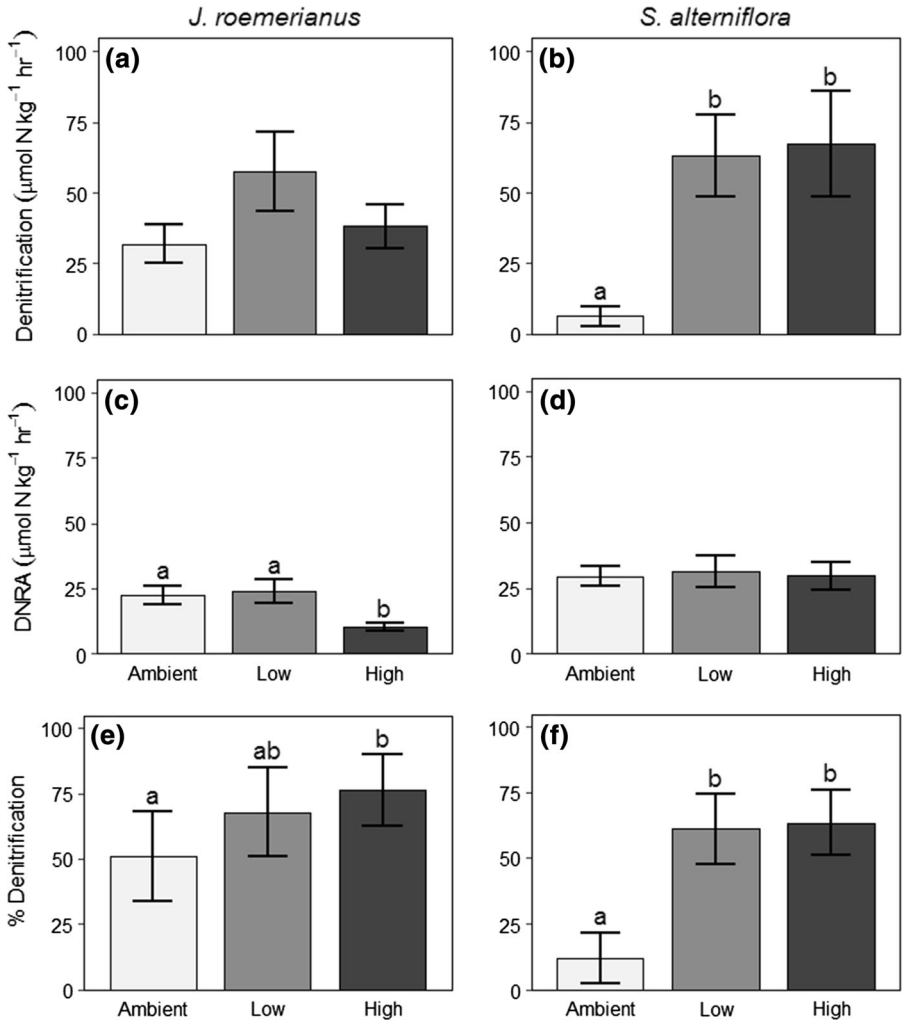

Fig. 4 Denitrification rates from **a** *J. roemerianus* and **b** *S. alterniflora* patches over the 2017–2018 study period (n = 3). Potential DNRA rates from **c** *J. roemerianus* and **d** *S. alterniflora* patches over the study period (n = 3). Percent denitrification contributed to dissimilatory nitrate reduction (DNRA + denitrification) from **e** *J. roemerianus* and **f**) *S. alterniflora* patches over the study period (n = 3). Error bars indicate ± 1 standard error. Denitrification was five-fold higher in *J. roemerianus* than *S. alterniflora* ambient plots (1-way ANOVA; p = 0.002), but DNRA rates were similar across ambient plots of both vegetation types (2-way ANOVA; p = 0.18). Different letters indicate significant differences between treatments within vegetation type (2-way ANOVA; $p < 0.05$)

nutrient addition plots of *J. roemerianus* ($F_{(2,23)}$ = 5.7, $p < 0.05$; Fig. 4c, d).

Denitrification varied temporally for both vegetation types, with lowest rates in summer (*J. roemerianus*: $F_{(2,24)}$ = 5.6, p = 0.01; *S. alterniflora:* $F_{(2,24)}$ = 4.4, $p < 0.05$; Table S1). There was no significant temporal effect on DNRA for either vegetation type, although rates appeared slightly lower ($\sim$ 20%) in summer (*J. roemerianus*: $F_{(2,23)}$ = 3.086, $p > 0.05$; *S. alterniflora:* $F_{(2,24)}$ = 3.626, $p > 0.05$; Table S1).

The contribution of denitrification to dissimilatory nitrate reduction (denitrification + DNRA) increased nearly six-fold in nutrient addition plots of *S. alterniflora* ($F_{(2,65)}$ = 4.385, $p < 0.05$; Fig. 4f), while denitrification contribution increased by nearly one-half in *J. roemerianus* high nutrient plots ($F_{(2,65)}$ = 4.385, $p < 0.05$; Fig. 4e). Denitrification contribution in *J. roemerianus* low addition plots was intermediate between ambient and high addition plots, but not significantly different from either ($F_{(2,65)}$ = 4.385, $p > 0.05$; Fig. 5).

Discussion

This study demonstrated that plant response to eutrophication had a significant impact on CO_2 fluxes and N-removal and retention in marshes. Fertilization increased *GPP* by one-third in *S. alterniflora* plots whereas there was no response in *J. roemerianus* plots (Fig. 5). Generally, marsh productivity is nutrient limited (Gallagher 1975; Haines 1979; Mendelssohn 1979; Buresh et al. 1980; Cargill and Jefferies 1980;

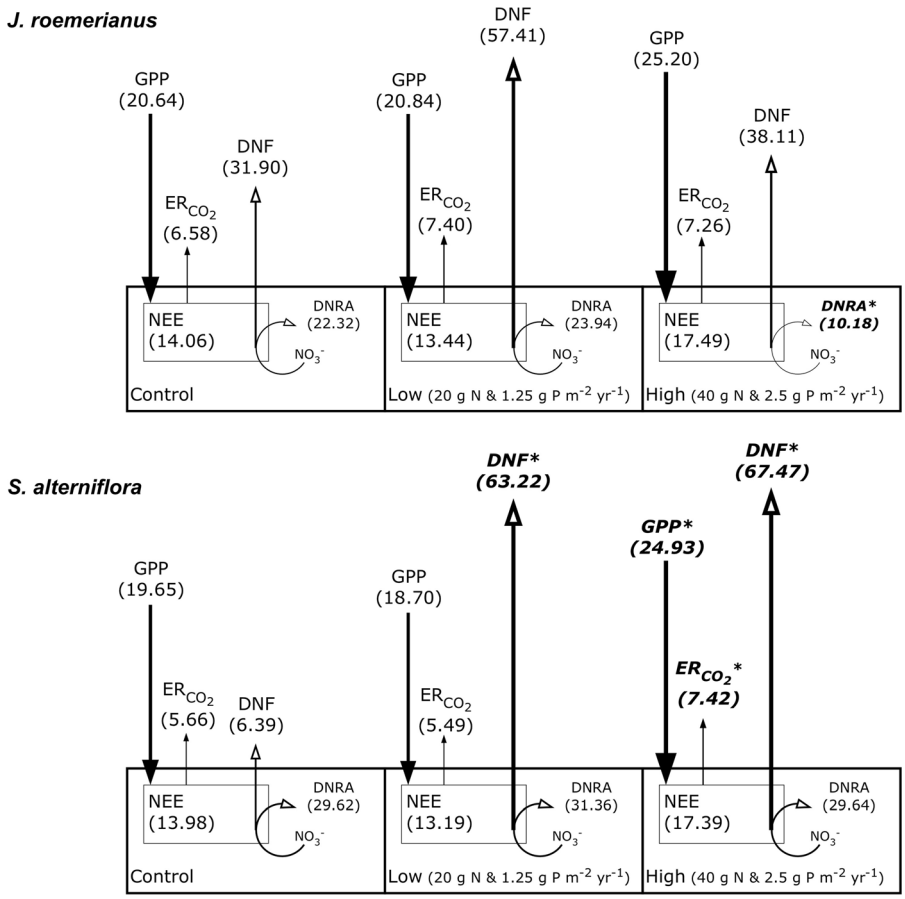

Fig. 5 Graphical summary representing mean *NEE*, *GPP*, and ER_{CO_2} (solid arrows) or denitrification (DNF) and DNRA (open arrows) from control and fertilized *J. roemerianus* and *S. alterniflora* plots (n = 3). Arrow direction indicates net gain (down) or net loss (up) from the marsh. Arrow sizes are relevant to the rates of losses or gains and bolded, italicized numbers with asterisks indicate significant differences between treatments ($p < 0.05$)

Cavalieri and Huang 1981; Delaune et al. 1986) and increased productivity in *S. alterniflora* plots indicates that in this anthropogenically impacted system, *S. alterniflora* may be more sensitive to eutrophication than *J. roemerianus.* Further, our study indicates that in this system *S. alterniflora* may be more sensitive to elevated nutrient loads than previously reported (Valiela et al. 1975; Darby and Turner 2008; Davis et al. 2017) where productivity response was only observed with nutrient loading rates nearly ten-fold higher ($\sim$ 400 g N m^{-2} yr^{-1}) than loading rates of the current study.

The differential response of plant productivity in *J. roemerianus* and *S. alterniflora* observed in this study is not unprecedented. N-enrichment has been shown to have a neutral to negative effect on *J. roemerianus* biomass and coverage across a range of N-enrichment levels and durations (Brewer 2003; Pennings et al. 2005; McFarlin et al. 2008; Hunter et al. 2015). Further, in mixed *S. alterniflora – J. roemerianus* marshes, *S. alterniflora* competitively utilizes N to increase biomass and coverage at the expense of *J. roemerianus* (Brewer 2003; Pennings et al. 2005; McFarlin et al. 2008). However, these studies all quantified productivity in biomass and coverage measurements, whereas our study demonstrates differential plant responses to fertilization through CO_2 fluxes.

Both vegetation types continued to be net C sinks with similar *NEE* before and after nutrient additions (Fig. 5). We did not observe a response of ER_{CO_2} that would be indicative of increased decomposition rates in *J. roemerianus,* however, ER_{CO_2} increased by one-third in *S. alterniflora* plots. This increase in respiration following fertilization is consistent with similar studies measuring respiration in *Spartina* marshes (Morris and Bradley 1999; Turner et al. 2009; Wigand et al. 2009; Martin et al. 2018), and could be indicative of enhanced N turnover in the subsurface sediment. Our study differs from these previous studies however, as we did not see an increase in sediment C loss with nutrient addition which suggests that at these loading rates and temporal duration of the study, C loss may be compensated for by the similar one-third increase in *GPP* in fertilized *S. alterniflora* plots.

We did not observe strong seasonality in primary productivity in either vegetation type, although *GPP* peaked in the early fall. However, the lowest H_2S concentrations were found during the growing season, while highest H_2S concentrations were measured following peak production in both vegetation types and during plant dormancy. These findings are consistent with Wilson et al. (2015) where H_2S concentrations where highest in winter months in *S. alterniflora* at our site and Miley and Kiene (2004) where concentrations were highest in fall months in a nearby monospecific *J. roemerianus* marsh. Our results differ, however, from findings of higher latitude New England marshes where growing seasons are shorter and sulfate reduction rates peak in summer months (Howarth and Teal 1979; Howarth et al. 1983; Hines et al. 1989). The temporal differences in H_2S across latitudes suggest that biogeochemical processes are at least partially controlled by temperature and/or duration of growing season.

H_2S concentrations were six-fold higher in *S. alterniflora* plots than *J. roemerianus* plots, which are consistent with previous measurements in the region (Miley and Kiene 2004; Wilson et al. 2015), and did not change with nutrient additions. Lower H_2S concentration in *J. roemerianus* plots has been attributed to greater belowground biomass associated with *J. roemerianus* compared to *S. alterniflora* and, thus, greater translocation of O_2 to the rhizosphere (Koretsky et al. 2008). Further, despite some of the highest sulfate reduction rates measured in salt marshes, Miley and Kiene (2004) suggested that the low H_2S concentrations in *J. roemerianus* marsh sediments were either due to rapid sulfide oxidation or precipitation into iron-sulfide minerals (Howarth 1979; Lord and Church 1983).

Considering sulfides suppress denitrification (Sorensen et al. 1980) and inhibit coupled nitrification–denitrification (Joye and Hollibaugh 1995), we anticipate lower H_2S concentrations in *J. roemerianus* control plots could account for the five-fold higher denitrification compared to *S. alterniflora* control plots. However, increases in productivity and ecosystem respiration in response to high nutrient inputs in *S. alterniflora* plots were concurrent with a substantial ten-fold increase in denitrification, suggesting a much greater response for removing excess N compared to plots dominated by *J. roemerianus* following nutrient additions. The magnitude of increase in denitrification in *S. alterniflora* is consistent with the findings of Hamersley and Howes (2005), who reported a seven-

fold increase in denitrification in response to N and P treatments in a *S. alterniflora* salt marsh.

Increases in *GPP* can increase root/rhizome translocation of O_2 to subsurface sediments (Koop-Jakobsen and Wenzhöfer 2015) alleviating H_2S toxicity (Sorensen et al. 1980) in the rhizosphere. However, our results suggest this was not the case, as we did not see a decrease in H_2S in *S. alterniflora* with enhanced *GPP*. It is possible that the increase in *GPP* in *S. alterniflora* plots resulted in higher labile C availability in subsurface sediments. Plants deliver labile C to soil microbial communities via roots and rhizomes (Spivak and Reeve 2015) which can stimulate heterotrophic processes including denitrification and DNRA, which are often C limited when carried out by heterotrophic microbes (Beauchamp et al. 1989; Kraft et al. 2011; Hardison et al. 2015). Thus, we consider that the greater C availability associated with higher *GPP* following nutrient enrichment likely promoted denitrification, rather than alleviation from H_2S toxicity.

Denitrification increased preferentially over DNRA following increased nutrient inputs in the highly sulfidic *S. alterniflora* sediments, though high accumulation of H_2S is expected to promote DNRA (Giblin et al. 2013). In fact, the percent contribution of denitrification to dissimilatory nitrate reduction (denitrification + DNRA) increased nearly six-fold from 11% in control plots to 63% in nutrient additions plots. Given that higher C/NO_3^- ratios typically favor DNRA (Tiedje 1982; Stremińska et al. 2012; Algar and Vallino 2014) the higher of contribution of denitrification to nitrate reduction following higher NO_3^- inputs were consistent with findings from previous reports (Stremińska et al. 2012; Hardison et al. 2015). This increasing trend of the contribution of denitrification to dissimilatory nitrate reduction is reflected in *J. roemerianus* sediments where denitrification contribution increased from 51 to 76% in the high nutrient treatments. However, this much smaller change in denitrification contribution found in *J. roemerianus* compared to *S. alterniflora* was attributed to a decline in DNRA rather than an increase in denitrification. Although the mechanisms for changes in denitrification contribution to nitrate reduction differed between the two vegetation types, it appears that energetically favored denitrification (Strohm et al. 2007; Kraft et al. 2014) is utilized at the expense of DNRA at this site when NO_3^- availability is enhanced (Fig. 5).

Despite the lower DNRA in nutrient amended plots, we still observed significant accumulation of porewater NH_4^+ with much higher concentrations in *J. roemerianus* sediments. Although we did not observe a response of ER_{CO_2} or changes in sediment C that would be indicative of increased decomposition rates, higher N production associated with high above ground biomass and high belowground turnover in *Juncus* could account for the accumulation of inorganic N in porewaters (Elsey-Quirk et al. 2011). Additionally, microbial assimilation and turnover, rather than dissimilatory processes, can account for 50 − 70% of NO_3^- processing in sediment (Hou et al. 2012). Given that plant type strongly influences belowground microbial community structure (Oliveira et al. 2012; Cleary et al. 2016, 2017; Liu et al. 2019), and that *J. romaeranus* and *S. alterniflora* have been shown to support different microbial communities at this (Mason et al. in review) and other sites (Rietl et al. 2016; Mavrodi et al. 2018), it is possible that differences in the microbial functional community affected rates of N assimilation and turnover in response to N loading. Although our study only focused on dissimilatory nitrate reduction pathways, future investigations should examine the role of vegetation on other N-cycling processes.

Our findings suggest that nutrient inputs may significantly impact *S. alterniflora* marshes more than *J. roemerianus* marshes, and that *S. alterniflora* marshes may be more sensitive to nutrient inputs than previously reported (Valiela et al. 1975; Darby and Turner 2008; Davis et al. 2017). Additionally, our C flux data support evidence of previous biomass work which suggests that productivity in *S. alterniflora* competitively utilizes N at the expense of *J. roemerianus* productivity in marshes where these two species coexist (Brewer 2003; Pennings et al. 2005; McFarlin et al. 2008). While N loads continue to increase in the biosphere with human activity (Galloway et al. 2008), it is important to understand how plant species-specific responses to stressors such as eutrophication could mediate important processes such as N-removal in marshes.

Acknowledgements This work was supported by the National Science Foundation (CBET #1438092, #1643486). We would like to thank Dr. J. A. Cherry whose comments and advice

greatly improved this manuscript and Dr. C. Staudhammer for statistical advice. We thank L. Linn for expertise in analytical analyses and use of DISL facilities. We also thank A. Kleihuizen and D. Tollette for numerous hours spent helping in the field and lab. Data is archived and publicly available at the NOAA National Centers for Environmental Information (NCEI). NCEI Accession Number is 0209238. A DOI will be issued once operations at the center resume following the COVID19 disruptions.

Compliance with ethical standards

Conflict of interest The authors declare that they have no conflict of interest.

References

Algar CK, Vallino JJ (2014) Predicting microbial nitrate reduction pathways in coastal sediments. Aquat Microb Ecol 71:223–238. https://doi.org/10.3354/ame01678

Alldred M, Baines SB (2016) Effects of wetland plants on denitrification rates: a meta-analysis. Ecol Appl 26:676–685

Babbin AR, Ward BB (2013) Controls on nitrogen loss processes in Chesapeake Bay sediments. Environ Sci Technol 47:4189–4196. https://doi.org/10.1021/es304842r

Beauchamp EG, Trevors JT, Paul JW (1989) Carbon sources for bacterial denitrification 10:113–142. https://doi.org/10.1007/978-1-4613-8847-0_3

Bilkovic DM, Mitchell M, Mason P, Duhring K (2016) The role of living shorelines as estuarine habitat conservation strategies. Coast Manag 44:161–174. https://doi.org/10.1080/08920753.2016.1160201

Boesch DF (2002) Challenges and opportunities for science in reducing nutrient over-enrichment of coastal ecosystems. Estuaries 25:886–900. https://doi.org/10.1007/BF02804914

Brewer JS (2003) Nitrogen addition does not reduce belowground competition in a salt marsh clonal plant community in Mississippi (USA). Plant Ecol 168:93–106. https://doi.org/10.1023/A:1024478714291

Bridgham SD, Megonigal JP, Keller JK et al (2006) The carbon balance of North American wetlands. Wetlands 26:889–916

Broome SW, Craft CB, Burchell MR (2019) Tidal marsh creation. In: Coastal Wetlands, Second. Elsevier, pp 789–816

Buresh RJ, Delaune RD, Patrick WH (1980) Nitrogen and phosphorus distribution and utilization by *Spartina alterniflora* in a Louisiana Gulf Coast marsh. Estuaries 3:111–121

Burgin AJ, Hamilton SK (2007) Have we overemphasized in aquatic removal of nitrate the role ecosystems? Pathways of denitrification review. Front Ecol Environ 5:89–96. https://doi.org/10.1890/1540-9295(2007)5[89:HWOTRO]2.0.CO;2

Cargill SM, Jefferies RL (1980) Nutrient limitation of primary production in sub-arctic salt marsh. J Appl Ecol 17:85–99. https://doi.org/10.1097/01.mlg.0000167980.08493.30

Cavalieri AJ, Huang AHC (1981) Accumulation of proline and glycinebetaine in *Spartina alterniflora* Loisel. in response to NaCl and nitrogen in the marsh. Ecology 49:224–228

Cleary DFR, Polónia ARM, Sousa AI et al (2016) Temporal dynamics of sediment bacterial communities in monospecific stands of *Juncus maritimus* and *Spartina maritima*. Plant Biol 18:824–834. https://doi.org/10.1111/plb.12459

Cleary DFR, Coelho FJRC, Oliveira V et al (2017) Sediment depth and habitat as predictors of the diversity and composition of sediment bacterial communities in an inter-tidal estuarine environment. Mar Ecol 38:1–15. https://doi.org/10.1111/maec.12411

Dalsgaard T, Thamdrup B, Canfield DE (2005) Anaerobic ammonium oxidation (anammox) in the marine environment. Res Microbiol 156:457–464. https://doi.org/10.1016/j.resmic.2005.01.011

Darby FA, Turner RE (2008) Below- and aboveground *Spartina alterniflora* production in a Louisiana salt marsh. Estuaries Coasts. https://doi.org/10.1007/s12237-007-9014-7

Davis J, Currin C, Morris JT (2017) Impacts of fertilization and tidal inundation on elevation change in microtidal, low relief salt marshes. Estuaries Coasts 40:1677–1687. https://doi.org/10.1007/s12237-017-0251-0

Delaune RD, Smith CJ, Sarafyan MN (1986) Nitrogen cycling in a freshwater marsh of *Panicum hemitomon* on the deltaic plain of the Mississippi River. J Ecol 74:249–256

Elsey-Quirk T, Seliskar DM, Gallagher JL (2011) Nitrogen pools of macrophyte species in a coastal lagoon salt marsh: implications for seasonal storage and dispersal. Estuaries Coasts 34:470–482. https://doi.org/10.1007/s12237-011-9379-5

Eyre BD, Rysgaard S, Dalsgaard T, Christensen PB (2002) Comparison of isotope pairing and N_2: Ar methods for measuring sediment denitrification-assumption, modifications, and implications. Estuaries 25:1077–1087. https://doi.org/10.1007/BF02692205

Fabricius KE (2005) Effects of terrestrial runoff on the ecology of corals and coral reefs: review and synthesis. Mar Pollut Bull 50:125–146. https://doi.org/10.1016/j.marpolbul.2004.11.028

Fisher J, Acreman MC (2004) Wetland nutrient removal: a review of the evidence. Hydrol Earth Syst Sci Discuss Eur Geosci Union 8:673–685

Fonselius S, Dyrssen D, Yhlen B (1983) Determination of hydrogen sulphide. In: Grasshof K (ed) Methods of Seawater Analysis, 3rd, Compl edn. Wiley-VCH, Weinheim, pp 91–100

Fox J, Weisberg S (2011) An R companion to applied regression, 2nd edn. Sage, Thousand Oaks, CA

Gallagher JL (1975) Effect of an ammonium nitrate pulse on the growth and elemental composition of natural stands of *Spartina alterniflora* and *Juncus roemerianus*. Am J Bot 62:644–648

Galloway JD, Townsend AR, Erisman JW, et al (2008) Transformation of the nitrogen cycle. Science 320:889–892. https://doi.org/10.1126/science.1136674

Giblin A, Tobias C, Song B et al (2013) The importance of dissimilatory nitrate reduction to ammonium (DNRA) in the nitrogen cycle of coastal ecosystems. Oceanography 26:124–131. https://doi.org/10.5670/oceanog.2013.54

Gittman RK, Peterson CH, Currin CA et al (2016) Living shorelines can enhance the nursery role of threatened estuarine habitats. Ecol Appl 26:249–263. https://doi.org/10.1890/14-0716.1/suppinfo

Grasshof K, Kremling K, Ehrhard M (1983) Methods of seawater analysis, 3rd, Compl edn. Wiley-VCH, Weinheim

Haines EB (1979) Growth dynamics of cordgrass, *Spartina alterniflora* Loisel., on control and sewage sludge fertilized plots in a Georgia salt marsh. Estuaries 2:50–53. https://doi.org/10.2307/1352040

Hamersley MR, Howes BL (2005) Coupled nitrification-denitrification measured in situ in a *Spartina alterniflora* marsh with a $^{15}NH_4^+$ tracer. Mar Ecol Prog Ser 299:123–135. https://doi.org/10.3354/meps299123

Hamme RC, Emerson SR (2004) The solubility of neon, nitrogen and argon in distilled water and seawater. Deep Res Part I Oceanogr Res Pap 51:1517–1528. https://doi.org/10.1016/j.dsr.2004.06.009

Hardison AK, Algar CK, Giblin AE, Rich JJ (2015) Influence of organic carbon and nitrate loading on partitioning between dissimilatory nitrate reduction to ammonium (DNRA) and N_2 production. Geochim Cosmochim Acta 164:146–160. https://doi.org/10.1016/j.gca.2015.04.049

Harris D, Horwath WR, Van KC (2001) Acid fumigation of soils to remove carbonates prior to total organic carbon or carbon-13 isotopic analysis. Soil Sci Soc Am 65:1853–1856

Hines ME, Knollmeyer SL, Tugel JB (1989) Sulfate reduction and other sedimentary biogeochemistry in a northern New England salt marsh. Limnol Oceanogr 34:578–590. https://doi.org/10.4319/lo.1989.34.3.0578

Holmes RM, Aminot A, Kerouel R et al (1999) A simple and precise method for measuring ammonium in marine and freshwater ecosystems. Can J Fish Aquat Sci 56:1801–1808

Hou L, Liu M, Carini SA, Gardner WS (2012) Transformation and fate of nitrate near the sediment-water interface of Copano Bay. Cont Shelf Res 35:86–94. https://doi.org/10.1016/j.csr.2012.01.004

Howarth RW (1979) Pyrite: its rapid formation in a salt marsh and its importance in ecosystem metabolism. Science 203:49–51

Howarth RW, Teal JM (1979) Sulfate reduction in a New England salt marsh. Limnol Oceanogr 24:999–1013. https://doi.org/10.1016/b978-0-12-114860-7.50024-7

Howarth RW, Marino R (2006) Nitrogen as the limiting nutrient for eutrophication in coastal marine ecosystems: evolving views over three decades. Limnol Oceanogr 51:364–376. https://doi.org/10.4319/lo.2006.51.1_part_2.0364

Howarth ARW, Giblin A, Gale J, et al (1983) Reduced sulfur compounds in the pore waters of a New England salt marsh. Environ Biogeochem 135–152

Hume NP, Fleming MS, Horne AJ (2002) Denitrification potential and carbon quality of four aquatic plants in wetland microcosms. Soil Sci Soc Am J 66:1706–1712. https://doi.org/10.2136/sssaj2002.1706

Hunter A, Cebrian J, Stutes JP et al (2015) Magnitude and trophic fate of black needlerush (*Juncus roemerianus*) productivity: does nutrient addition matter? Wetlands 35:401–417. https://doi.org/10.1007/s13157-014-0611-5

Joye SB, Hollibaugh JT (1995) Influence of sulfide inhibition of nitrification on nitrogen regeneration in sediments. Science 270:623–625

Kana TM, Darkangelo C, Hunt MD et al (1994) Membrane inlet mass spectrometer for rapid high-precision determination of N_2, O_2, and Ar in environmental water samples. Anal Chem 66:4166–4170. https://doi.org/10.1021/ac00095a009

Knowles R (1982) Denitrification. Microbiol Rev 46:43–70. https://doi.org/10.1016/0968-0004(76)90171-7

Koop-Jakobsen K, Wenzhöfer F (2015) The dynamics of plant-mediated sediment oxygenation in *Spartina anglica* rhizospheres—a planar optode study. Estuaries Coasts 38:951–963. https://doi.org/10.1007/s12237-014-9861-y

Koretsky CM, Haveman M, Cuellar A et al (2008) Influence of *Spartina* and *Juncus* on saltmarsh sediments: I. pore water geochemistry. Chem Geol 255:87–99. https://doi.org/10.1016/j.chemgeo.2008.06.013

Kraft B, Strous M, Tegetmeyer HE (2011) Microbial nitrate respiration—Genes, enzymes and environmental distribution. J Biotechnol 155:104–117. https://doi.org/10.1016/j.jbiotec.2010.12.025

Kraft B, Tegetmeyer HE, Sharma R, et al (2014) The environmental controls that govern the end product of bacterial nitrate respiration. Science 345:676–679. https://doi.org/10.1126/science.1254070

Liu Y, Luo M, Ye R et al (2019) Impacts of the rhizosphere effect and plant species on organic carbon mineralization rates and pathways, and bacterial community composition in a tidal marsh. FEMS Microbiol Ecol 95:1–15. https://doi.org/10.1093/femsec/fiz120

Lord CJ, Church TM (1983) The geochemistry of salt marshes: sedimentary ion diffusion, sulfate reduction, and pyritization. Geochim Cosmochim Acta 47:1381–1391

Martin RM, Wigand C, Elmstrom E et al (2018) Long-term nutrient addition increases respiration and nitrous oxide emissions in a New England salt marsh. Ecol Evol 8:4958–4966. https://doi.org/10.1002/ece3.3955

Mason OU, Chanton P, Knobbe LN, et al (in review) New insights into the influence of plant and microbial diversity on denitrification rates in a salt marsh. Microb Ecol

Mavrodi OV, Jung CM, Eberly JO et al (2018) Rhizosphere microbial communities of *Spartina alterniflora* and *Juncus roemerianus* from restored and natural tidal marshes on Deer Island, Mississippi. Front Microbiol 9:1–13. https://doi.org/10.3389/fmicb.2018.03049

McFarlin CR, Brewer JS, Buck TL, Pennings SC (2008) Impact of fertilization on a salt marsh food web in Georgia. Estuaries Coasts 31:313–325. https://doi.org/10.1007/s12237-008-9036-9

Mendelssohn IA (1979) The influence of nitrogen level, form and application method on the growth response of *Spartina alterniflora* in North Carolina. Estuaries 2:106–112. https://doi.org/10.2307/1351634

Miley GA, Kiene RP (2004) Sulfate reduction and porewater chemistry in a Gulf Coast *Juncus roemerianus* (Needlerush) marsh. Estuaries 27:472–481. https://doi.org/10.1007/BF02803539

Morris JT, Bradley PM (1999) Effects of nutrient loading on the carbon balance of coastal wetland sediments. Limnol Oceanogr 44:699–702. https://doi.org/10.4319/lo.1999.44.3.0699

National Atmospheric Deposition Program (NRSP-3) (2016) NADP Program Office, Wisconsin State Laboratory of Hygiene. 465 Henry Mail, Madison, WI 53706

Neubauer SC (2013) Ecosystem responses of a tidal freshwater marsh experiencing saltwater intrusion and altered hydrology. Estuaries Coasts 36:491–507. https://doi.org/10.1007/s12237-011-9455-x

Nielsen LP (1992) Denitrification in sediment determined from nitrogen isotope pairing technique. FEMS Microbiol Lett 86:357–362

Nixon SW (1995) Coastal marine eutrophication: a definition, social causes, and future concerns. Ophelia 41:199–219

Oliveira V, Santos AL, Coelho F et al (2010) Effects of monospecific banks of salt marsh vegetation on sediment bacterial communities. Microb Ecol 60:167–179. https://doi.org/10.1007/s00248-010-9678-6

Oliveira V, Santos AL, Aguiar C et al (2012) Prokaryotes in salt marsh sediments of Ria de Aveiro: effects of halophyte vegetation on abundance and diversity. Estuar Coast Shelf Sci 110:61–68. https://doi.org/10.1016/j.ecss.2012.03.013

Pennings SC, Clark CM, Cleland EE et al (2005) Do individual plant species show predictable responses to nitrogen addition across multiple experiments? Oikos 110:547–555. https://doi.org/10.1111/j.0030-1299.2005.13792.x

Pinheiro J, Bates D, DebRoy S, et al (2018) Linear and nonlinear mixed effects models. R Package version 31–137

Rabalais NN, Turner RE, Wiseman WJ (2002) Gulf of Mexico hypoxia, A.K.A. "The Dead Zone". Annu Rev Ecol Syst 33:235–263. https://doi.org/10.1146/annurev.ecolsys.33.010802.150513

Rietl AJ, Overlander ME, Nyman AJ, Jackson CR (2016) Microbial community composition and extracellular enzyme activities associated with *Juncus roemerianus* and *Spartina alterniflora* vegetated sediments in Louisiana saltmarshes. Microb Ecol 71:290–303. https://doi.org/10.1007/s00248-015-0651-2

Schnetger B, Lehners C (2014) Determination of nitrate plus nitrite in small volume marine water samples using vanadium(III)chloride as a reduction agent. Mar Chem 160:91–98. https://doi.org/10.1016/j.marchem.2014.01.010

Smith VH (2003) Eutrophication of freshwater and coastal marine ecosystems: a global problem. Environ Sci Pollut Res 10:126–139. https://doi.org/10.1065/espr2002.12.142

Smith KA, Caffrey JM (2009) The effects of human activities and extreme meteorological events on sediment nitrogen dynamics in an urban estuary, Escambia Bay, Florida, USA. Hydrobiologia 627:67–85. https://doi.org/10.1007/s10750-009-9716-x

Smith VH, Wood SA, McBride CG et al (2016) Phosphorus and nitrogen loading restraints are essential for successful eutrophication control of Lake Rotorua, New Zealand. Inl Waters 6:273–283. https://doi.org/10.5268/IW-6.2.998

Sorensen J, Tiedje JM, Firestone RB (1980) Inhibition by sulfide of nitric and nitrous oxide reduction by denitrifying *Pseudomonas fluorescens*. Appl Environ Microbiol 39:105–108

Spivak AC, Reeve J (2015) Rapid cycling of recently fixed carbon in a *Spartina alterniflora* system: a stable isotope tracer experiment. Biogeochemistry 125:97–114. https://doi.org/10.1007/s10533-015-0115-2

Stremińska MA, Felgate H, Rowley G et al (2012) Nitrous oxide production in soil isolates of nitrate-ammonifying bacteria. Environ Microbiol Rep 4:66–71. https://doi.org/10.1111/j.1758-2229.2011.00302.x

Strohm TO, Griffin B, Zumft WG, Schink B (2007) Growth yields in bacterial denitrification and nitrate ammonification. Appl Environ Microbiol 73:1420–1424. https://doi.org/10.1128/AEM.02508-06

Thamdrup B, Dalsgaard T (2002) Production of N_2 through anaerobic ammonium oxidation coupled to nitrate reduction in marine sediments. Appl Environ Microbiol 68:1312–1318. https://doi.org/10.1128/AEM.68.3.1312

Tiedje JM (1982) Denitrification. In: Page AL (ed) Methods of soil analysis: Part 2. Chemical and Microbiological properties, 2nd edn. Agron. Monogr., Madison, WI, pp 1011–1026

Turner RE, Howes BL, Teal JM et al (2009) Salt marshes and eutrophication: an unsustainable outcome. Limnol Oceanogr 54:1634–1642. https://doi.org/10.4319/lo.2009.54.5.1634

Twilley RR, Cowan J, Miller-Way T et al (1999) Benthic nutrient fluxes in selected estuaries in the Gulf of Mexico. In: Bianchi TS, Pennock JR, Twilley RR (eds) Biogeochemistry of Gulf of Mexico Estuaries. Wiley-Liss, New York, pp 163–209

Valiela I, Cole ML (2002) Comparative evidence that salt marshes and mangroves may protect seagrass meadows from land-derived nitrogen loads. Ecosystems 5:92–102. https://doi.org/10.1007/s10021-001-0058-4

Valiela I, Teal JM, Sass WJ (1975) Production and dynamics of salt marsh vegetation and the effects of experimental treatment with sewage sludge: biomass, production and species composition. Br Ecol Soc 12:973–981

Vitousek PM, Aber JD, Howarth RW et al (1997) Human alteration of the global nitrogen cycle. Ecol Soc Am 7:737–750

Wigand C, Brennan P, Stolt M et al (2009) Soil respiration rates in coastal marshes subject to increasing watershed nitrogen loads in southern New England, USA. Wetlands 29:952–963

Wilson BJ, Mortazavi B, Kiene RP (2015) Spatial and temporal variability in carbon dioxide and methane exchange at three coastal marshes along a salinity gradient in a northern Gulf of Mexico estuary. Biogeochemistry 123:329–347. https://doi.org/10.1007/s10533-015-0085-4

Yin G, Hou L, Liu M et al (2014) A novel membrane inlet mass spectrometer method to measure $^{15}NH_4^+$ for isotope-enrichment experiments in aquatic ecosystems. Environ Sci Technol 48:9555–9562. https://doi.org/10.1021/es501261s